

Wave propagation at high dissociation temperatures

P. A. Blythe



Received: 30 May 2008 / Accepted: 17 July 2008 / Published online: 12 August 2008
© Springer Science+Business Media B.V. 2008

Abstract Waves in ideal dissociating gases are examined in the limit of large dissociation temperatures. Both strong shock waves and weak finite-amplitude signalling problems are considered. The shock analysis is based on the Freeman limit, and an extension to higher Mach numbers is given. Even small-amplitude near-field theories, which are concerned with times comparable to the signal scale, can contain nonlinear exponential terms when the dissociation temperature is large. A corresponding endothermic Clarke equation is derived and solutions are determined in the Newtonian limit. Far-field theory, involving both convective and chemical nonlinearities, is also discussed. Suitable high-frequency solutions are obtained, together with results for the evolution of the shock path and the decay of the signal amplitude.

Keywords Endothermic Clarke equation · Ideal dissociating gases · Nonlinear far field theory · Shock structure

1 Introduction

The concept of an ideal dissociating gas was introduced by Lighthill [1] who showed that in the equilibrium limit the behavior of many dissociating gases was essentially controlled by two parameters: a characteristic dissociation density ρ'_D , and a characteristic dissociation temperature Θ'_D . This observation was supplemented by a simple model for the internal energy content. As observed by Freeman [2], addition of a suitable rate law enables the approach to be extended in a straightforward manner to nonequilibrium flows. Use of the ideal model allows focus to be placed on the principal features of a broad class of aerothermodynamic problems. Early applications were discussed by Clarke and McChesney [3, Chap. 6] and by Vincenti and Kruger [4, Chap. VIII]. Characteristic dimensionless values ρ_D and Θ_D are usually large and result in finite levels of the atomic mass fraction. In this paper, the analysis is concerned with wave propagation in an ideal dissociating gas when the dissociation temperature is large. A description of this limit requires inclusion of exponential terms that are not present in either classical linear theories nor in some standard far-field theories that incorporate convective nonlinearities.

Properties of the ideal dissociating gas are briefly reviewed in Sect. 2, where a simple extension is made with respect to the internal energy model. Details of the equilibrium limit, the relevant high- and low-frequency sound

P. A. Blythe (✉)

Department of Mechanical Engineering and Mechanics, Lehigh University, 19 Memorial Drive W., Bethlehem, PA 18015, USA
e-mail: pab0@lehigh.edu

speeds, and the characteristic form of the governing non-equilibrium equations are also given in Sect. 2. The high-frequency sound speed corresponds to the frozen limit in which the dissociation mass fraction remains constant, and the low-frequency sound speed is defined by thermodynamic equilibrium.

In part, the early paper by Freeman [2] was concerned with the structure of the dissociation region behind strong shock waves, and an analysis was given for the limit in which there is a balance between the dissociation energy and the kinetic energy. For this case, although the dissociation temperature is large compared with the upstream temperature, it is not large compared with the temperature downstream of the shock. Nevertheless, the corresponding dissociation density is still large compared with downstream levels. A discussion based on the latter limit is presented in Sect. 3 where a comparison is made with numerical results. It is shown that the value of the Freeman parameter $\mu_F = \frac{1}{2}U'^2/R\Theta'_D$, where U' is the shock speed and R is the molecular gas constant, provides a clear distinction between the controlling decay mechanisms associated with dissociation and recombination.

An excellent early treatment of relaxation effects in waves of finite amplitude was given by Lighthill [5], where a discussion of the far-field balance between weak convective steepening and diffusive effects due to the rate process was presented; these flows are controlled by Burgers' equation. Simple linear near-field theory, which does not include convective steepening or exponential nonlinearities associated with the chemistry, leads to a third-order wave equation in which the high-frequency propagation speed is defined by the frozen limit, and the low-frequency speed by the equilibrium value. Numerous studies of the properties of this equation are available in the literature; see [3, Chap. 6; 4, Chap. VIII; 6]. At large dissociation temperatures, however, modifications of this linear equation are required. A related analysis for the propagation of small disturbances in a combustible mixture at large activation energies has been described by Clarke [7]. He showed that even in the near-field the low-frequency operator is now applied to an exponentially nonlinear term and that the low-frequency wave speed corresponds to the isothermal sound speed. By using a similar strategy for an ideal dissociating gas, at large dissociation temperatures, a result corresponding to the Clarke equation can be obtained. Details are given in Sect. 4. For combustion the process is exothermic, but for dissociation the overall process is endothermic. This leads to an obvious sign difference between the two equations; a compressive disturbance in the combustion case can lead to ignition, but for dissociation the wave amplitude is weakened by heat loss.

Direct solutions of the Clarke equation, or its endothermic counterpart, do not seem to be possible. Numerical investigations of the exothermic case can be found in [8] and in [9], where local structures based on coordinate expansions were obtained. In the Newtonian limit, however, an analytical approach was developed by Blythe and Crighton [10]. For this limit the two sound speeds are close together and considerable progress can be made. Related approximations for relaxing gases, without the exponential nonlinearity, can be found in [11–13]. Use of this limit is discussed in Sect. 4 for the ideal dissociating gas. Even at large dissociation temperatures it is found that, as in [11], part of the near field is now governed by the telegraph equation, and the relevant large time behavior of this equation is described.

High-activation-energy far-field theories including convective nonlinearities have been outlined in [14, 15]. A corresponding analysis for the ideal dissociating gas is presented in Sect. 5 for a high-frequency limit in which both convective and chemical nonlinearities are important. The solution of the resulting evolution equation is obtained for a general input signal, and implications for shock formation and propagation, together with asymptotic decay laws for the shock strength, are determined.

2 Thermodynamic model and conservation laws

The ideal dissociating-gas model was originally developed by Lighthill [1] for the equilibrium case and extended to non-equilibrium situations by Freeman [2]. For the assumed chemistry,



the equilibrium atomic mass fraction α_e is defined by

$$\frac{\alpha_e^2}{1 - \alpha_e} = \frac{\rho'_D}{\rho'} \exp(-D'_{\text{en}}/kT') \quad (2.2)$$

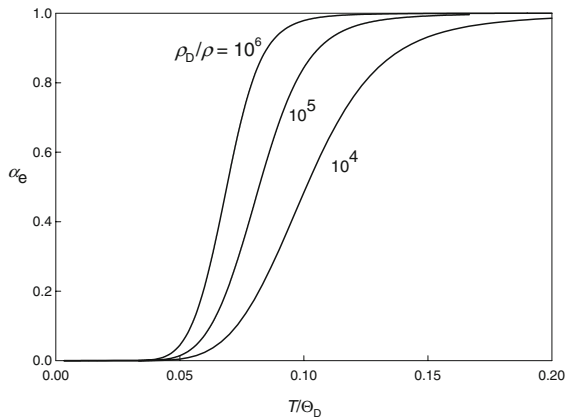


Fig. 1 Equilibrium curves for various densities

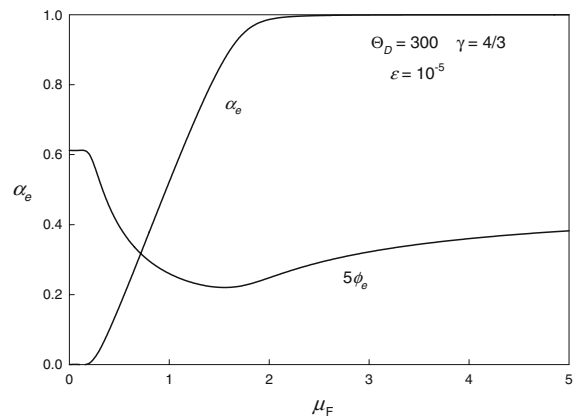


Fig. 2 Equilibrium shock values

where D'_{en} is the dissociation energy, k is Boltzmann’s constant, T' is the gas temperature, and ρ' is the gas density. In (2.2) $\rho'_D(T')$ is a characteristic density which, for the ideal dissociating gas, is assumed constant; the variation with temperature was discussed in [1]. In (2.2) it is also convenient to set

$$\Theta'_D = D'_{en}/k, \tag{2.3}$$

where Θ'_D is a characteristic dissociation temperature. When compared with standard atmospheric conditions (ρ'_{atm}, T'_{atm}), dimensionless values are

Gas	$\rho_{Da} = \rho'_D/\rho'_{atm}$	$\Theta_{Da} = \Theta'_D/T'_{atm}$
O ₂	1.2×10^5	200
N ₂	1.2×10^5	380

(Note that ρ'_{atm} corresponds to the specific gas listed.) Typical equilibrium mass fractions are shown in Fig. 1.

In the general non-equilibrium case the atomic mass fraction must be determined through the rate law and appropriate thermodynamic models. For the mixture of atoms and molecules, the state equation is

$$p' = R\rho'T'(1 + \alpha) \tag{2.4}$$

where p' is the pressure, α is the actual atomic mass fraction, $R = k/2m$ is the molecular gas constant, and m is the atomic mass. Assuming that the translational and rotational modes are fully excited and in thermodynamic equilibrium, the specific internal energy can be written for a dissociating diatomic gas as

$$e' = \left(\frac{5}{2} + \frac{\alpha}{2}\right)RT' + (1 - \alpha)e'_{vib} + R\Theta'_D\alpha, \tag{2.5}$$

where e'_{vib} is the vibrational energy contribution. For simplicity, Lighthill assumed that this internal mode was also in thermodynamic equilibrium (the time scale for adjustment of the vibrational mode is typically much less than that required to reach the equilibrium balance between dissociation and recombination), and that it could be treated as half-excited with

$$e'_{vib} = \frac{1}{2}RT'.$$

This leads to

$$e' = 3RT' + R\Theta'_D\alpha.$$

At very elevated temperatures, a more realistic assumption may be that of full excitation with $e'_{vib} = RT'$, which gives

$$e' = \left(\frac{7}{2} - \frac{\alpha}{2}\right)RT' + R\Theta'_D\alpha.$$

Here, for convenience, (2.5) is re-written as

$$e' = \frac{1}{\gamma - 1} RT' + R\Theta'_D \alpha, \quad (2.6)$$

where, in general, the effective specific heat ratio $\gamma = \gamma(T', \alpha)$. For the classical ideal dissociating gas $\gamma = 4/3$. The fully excited assumption also yields $\gamma = 4/3$ for $\alpha = 1$, $\gamma = 17/14$ for $\alpha = 1/2$, and $\gamma = 9/7$ for $\alpha = 0$. There is little difference among these values and, in the spirit of the ideal dissociating gas approximation, γ is taken as constant throughout this paper.

For either the frozen or the equilibrium limits, it is permissible to define the specific entropy s' by

$$T' ds' = de' + p' d(1/\rho'). \quad (2.7)$$

When describing the evolution of disturbances in a dissociating gas, one can anticipate that two particular sound speeds will be of interest. Specifically, these are the frozen sound speed defined by

$$a'^2 = \left. \frac{\partial p'}{\partial \rho'} \right|_{s', \alpha} = \{\gamma + (\gamma - 1)\alpha\} \frac{p'}{\rho'}, \quad (2.8)$$

and the equilibrium sound speed given by

$$a_e'^2 = \left. \frac{\partial p'}{\partial \rho'} \right|_{s', \alpha = \alpha_e} = \left\{ \frac{1 + 2 \frac{T'}{\Theta'_D} + \frac{2\gamma + 3(\gamma - 1)\alpha_e - (\gamma - 1)\alpha_e^3}{(\gamma - 1)\alpha_e(1 - \alpha_e^2)} \frac{T'^2}{\Theta_D'^2}}{1 + \left\{ \frac{2 - \alpha_e}{(\gamma - 1)\alpha_e(1 - \alpha_e)} \right\} \frac{T'^2}{\Theta_D'^2}} \right\} \frac{p'}{\rho'} \quad (2.9)$$

(see [4, p. 261]). Inspection of (2.9) indicates that, when $\Theta'_D \gg T'$,

$$a_e' \rightarrow \sqrt{\frac{p'}{\rho'}}, \quad (2.10)$$

which corresponds to the isothermal frozen sound speed, i.e.,

$$a_T' = \left(\sqrt{\frac{\partial p'}{\partial \rho'}} \right) \Big|_{T', \alpha} = \sqrt{\frac{p'}{\rho'}}. \quad (2.11)$$

As noted above, a description of the non-equilibrium process requires specification of a suitable rate law. Freeman [2] adopted the model

$$\partial_{t'} \alpha = C \rho' T'^{-n} \left\{ (1 - \alpha) \exp(-\Theta'_D/T') - (\rho'/\rho'_D) \alpha^2 \right\}, \quad (2.12)$$

where $\partial_{t'}$ denotes the one-dimensional convective operator

$$\partial_{t'} \equiv \frac{\partial}{\partial t'} + u' \frac{\partial}{\partial x'} \quad (2.13)$$

in which u' is the gas velocity in the x' -direction and t' denotes time. Throughout the present paper the exponent n in the rate equation is taken to be zero. The group

$$C \rho' (1 - \alpha) \exp(-\Theta'_D/T')$$

represents the dissociation rate, and

$$C \rho' (\rho'/\rho'_D) \alpha^2$$

is the recombination rate. A balance between these rates leads to the equilibrium law (2.2).

For one-dimensional unsteady flow, conservation of mass, momentum, and energy requires that

$$\partial_{t'} \rho' + \rho' u_{x'} = 0, \quad \partial_{t'} u' + \rho'^{-1} p_{x'} = 0, \quad \partial_{t'} e' + p' \partial_{t'} (\rho'^{-1}) = 0, \quad (2.14)$$

where the subscript x' denotes differentiation with respect to x' . The equations are re-expressed in dimensionless form by introducing suitable reference quantities

$$p'_r, \rho'_r, T'_r = p'_r/R\rho'_r, \quad e'_r = p'_r/\rho'_r, \quad \text{and} \quad u'_r = \sqrt{p'_r/\rho'_r}, \quad (2.15)$$

together with a time scale t'_r defined by the applied signal. Dimensionless time and distance scales are

$$t = t'/t'_r, \quad x = x'/u'_r t'_r, \quad (2.16)$$

and the equations can be written in dimensionless characteristic form as

$$\begin{aligned} \partial_{\pm} p \pm \rho a \partial_{\pm} u &= -b\rho\Theta_D\Omega, \\ \partial_t p - a^2 \partial_t \rho &= -b\rho\Theta_D\Omega, \\ \partial_t \alpha &= \Omega = \lambda\rho \left\{ (1 - \alpha) \exp(-\Theta_D/T) - \varepsilon\rho\alpha^2 \right\}. \end{aligned} \quad (2.17)$$

Here

$$b = \frac{1}{\rho\Theta_D} \frac{\partial e/\partial\alpha}{\partial e/\partial p} = (\gamma - 1)(1 + \alpha) - (T/\Theta_D), \quad (2.18)$$

$$\Theta_D = R\rho'_r\Theta'_D/p'_r, \quad \varepsilon = \rho'_r/\rho'_D, \quad \lambda = C'\rho'_r t'_r,$$

and λ is the dimensionless rate parameter. The characteristic operators in (2.17) are

$$\partial_{\pm} \equiv \frac{\partial}{\partial t} + (u \pm a) \frac{\partial}{\partial x}. \quad (2.19)$$

Corresponding to (2.4), the dimensionless equation of state is

$$p = \rho T (1 + \alpha). \quad (2.20)$$

3 Shock structure

3.1 The Freeman limit

The non-equilibrium zone behind a strong shock wave in an ideal dissociating gas was examined by Freeman [2] for the large-dissociation-energy limit. Specifically, Freeman considered the case when

$$\mu_F = \frac{mU'^2}{D'_{\text{en}}} = O(1), \quad (3.1)$$

where U' is the shock speed. Numerical solutions were presented for various μ_F and inverse dissociation densities ε . A similar limit is considered in this section where an analysis is given for the case $\mu_F = O(1)$ with $\varepsilon \ll 1$. Upstream of the shock front it is assumed that equilibrium conditions hold and, subject to (3.1), it follows that the equilibrium mass fraction is exponentially small in this region and can be ignored. If the reference state (2.15) for the dependent variables is defined by conditions in the upstream region, the relation (3.1) can be re-expressed as

$$\mu_F = \frac{\gamma M_1^2}{2\Theta_D}, \quad (3.2)$$

where M_1 is the shock Mach number based on the upstream frozen sound speed. Equivalently, $\Theta_D = O(M_1^2)$. Using the upstream state as the reference condition, the steady one-dimensional conservation relations reduce to

$$\rho u = \gamma^{\frac{1}{2}} M_1, \quad p + \rho u^2 = 1 + \gamma M_1^2, \quad \frac{\Gamma}{\Gamma - 1} \frac{p}{\rho} + \Theta_D \alpha + \frac{1}{2} u^2 = \frac{\gamma}{\gamma - 1} + \frac{\gamma}{2} M_1^2, \quad (3.3)$$

where

$$\Gamma = \gamma + (\gamma - 1)\alpha \quad (3.4)$$

is the frozen specific heat ratio. By viewing $q = \Theta_D \alpha$ as the heat extraction (see [16]), the usual Rayleigh-line relation holds, i.e. using the first two relations in (3.3)

$$p - 1 = \gamma M_1^2 (1 - \rho^{-1}). \tag{3.5}$$

Similarly, the Hugoniot relation connecting p , ρ , and q can be written

$$p = \frac{2q + \rho^{-1} - ((\gamma + 1)/(\gamma - 1))}{1 - ((\Gamma + 1)/(\Gamma - 1)) \rho^{-1}}. \tag{3.6}$$

From (3.2), (3.5), and (3.6), with $\Theta_D \gg 1$, it follows that within the subsonic relaxation zone behind the strong shock the leading approximations to the flow variables can be written

$$p = \gamma M_1^2 \frac{1 + D}{\Gamma + 1}, \quad \frac{u}{\gamma^{\frac{1}{2}} M_1} = \rho^{-1} = \frac{\Gamma - D}{\Gamma + 1}, \quad \frac{T}{\gamma M_1^2} = \phi = \frac{(\Gamma - D)(1 + D)}{(\Gamma + 1)^2 (1 + \alpha)}, \tag{3.7}$$

where

$$D = \sqrt{1 + (\Gamma^2 - 1)(\alpha/\mu_F)}. \tag{3.8}$$

Prior to evaluating the non-equilibrium solution, it is helpful to obtain the equilibrium solutions for various μ_F at a fixed value of Θ_D . These are displayed in Fig. 2. Note that μ_F is a monotonically increasing function of the shock Mach number at fixed Θ_D . In Fig. 2

$$\phi(\alpha_e) = \phi_e = \frac{T(\alpha_e)}{\gamma M_1^2} = \frac{(\Gamma - D)(1 + D)}{(\Gamma + 1)^2 (1 + \alpha)} \Big|_{\alpha=\alpha_e} \tag{3.9}$$

is a scaled temperature. The equilibrium solutions satisfy

$$\frac{\alpha_e^2}{1 - \alpha_e} = \frac{1}{\varepsilon \rho_e} \exp(-1/2\mu_F \phi_e), \tag{3.10}$$

where ρ_e is defined by (3.7) with $\alpha = \alpha_e$. Clearly, for $\mu_F > 2$ the equilibrium state corresponds to complete dissociation with $\alpha_e \approx 1$. For this limit, it is seen from (3.10) that

$$\alpha_e = 1 - \varepsilon \rho_e (1) \exp(1/2\mu_F \phi_e(1)) + O(\varepsilon^2). \tag{3.11}$$

The behavior of the temperature ϕ_e seems surprising, but it is readily established that

$$\phi_e \rightarrow \frac{2(\gamma - 1)}{(\gamma + 1)^2} \quad \text{as } \alpha_e \rightarrow 0, \quad \text{and} \quad \phi_e \sim \frac{(\gamma - 1)}{2\gamma^2} \left\{ 1 - \frac{\gamma(2 - \gamma)}{\mu_F} + O\left(\varepsilon, \mu_F^{-2}\right) \dots \right\} \quad \text{as } \varepsilon, \mu_F^{-1} \rightarrow 0.$$

Both these results are consistent with Fig. 2.

The dimensionless form of the rate law for steady flow is

$$u \frac{d\alpha}{dx} = \lambda \rho \left\{ (1 - \alpha) \exp(-1/2\mu_F \phi) - \varepsilon \rho \alpha^2 \right\}, \tag{3.12}$$

and the dimensionless dissociation rate

$$\lambda \rho (1 - \alpha) \exp(-1/2\mu_F \phi),$$

vanishes when either $\alpha \rightarrow 1$ or $\phi \rightarrow 0$. The distinction between these limits has important consequences for the asymptotic analysis, and the results shown in Fig. 2 suggest that the former limit is the appropriate one for $\mu_F \gg 1$. Inspection of (3.7) indicates that $\phi = 0$ occurs when $D = \Gamma$, which is equivalent to $\alpha = \mu_F$. Because α increases monotonically behind the shock wave (dissociation can be neglected upstream of the shock), it follows that

$$\begin{aligned} \alpha = 1 & \text{ would occur prior to } \phi = 0 \text{ for } \mu_F > 1; \\ \phi = 0 & \text{ would occur prior to } \alpha = 1 \text{ for } \mu_F < 1. \end{aligned} \tag{3.13}$$

Equilibrium, however, can be attained prior to either of these events.

3.2 Freeman parameter $\mu_F > 1$, large dissociation density $\varepsilon^{-1} \gg 1$

Here it is assumed that the rate parameter λ and a factor $\gamma^{\frac{1}{2}} M_1$ have been incorporated into the distance coordinate x , whose origin is at the shock. As $\varepsilon \rightarrow 0$, with $\mu_F = O(1)$, the basic expansion for $x = O(1)$ is

$$\alpha = \alpha_0(x) + \varepsilon \alpha_1(x) + \dots \quad (3.14)$$

Using (3.12), with $\alpha = 0$ at $x = 0$, gives the first-order solution

$$x = \int_0^{\alpha_0} \frac{\exp(1/2\mu_F\phi(s))}{\rho^2(s)(1-s)} ds = \int_0^{\alpha_0} \frac{A(s)}{(1-s)} ds, \quad (3.15)$$

where $\rho(\alpha_0)$, $\phi(\alpha_0)$ are defined by (3.7) with $\alpha = \alpha_0$. With $\mu_F > 1$, the limiting behavior as $x \rightarrow \infty$ is associated with $\alpha_0 \rightarrow 1$ and it can be established that

$$\alpha_0 \sim 1 - k_0 \exp(-\omega_0 x) + \dots, \quad (3.16)$$

where

$$\omega_0 = 1/A(1), \quad k_0 = \exp(\omega_0 K_0), \quad \text{and} \quad K_0 = \int_0^1 \frac{A(s) - A(1)}{1-s} ds. \quad (3.17)$$

Similarly, it can be established that

$$\alpha_1 = -\frac{1 - \alpha_0}{A(\alpha_0)} \int_0^{\alpha_0} \frac{B(s)}{(1-s)^2} ds, \quad (3.18)$$

where

$$B(\alpha) = \alpha^2 \rho^3(\alpha) A^2(\alpha). \quad (3.19)$$

Straightforward calculations indicate that as $x \rightarrow \infty$ ($\alpha_0 \rightarrow 1$)

$$\alpha_1 \sim -\frac{B(1)}{A(1)} + k_0 \left(\frac{B'(1)}{A(1)} \omega_0 x - \omega_0 K_0 \frac{B'(1)}{A(1)} + f_1 \right) \exp(-\omega_0 x) + \dots, \quad (3.20)$$

where

$$f_1 = -\frac{B(1)(A'(1) - A(1))}{A^2(1)} + \frac{1}{A(1)} \int_0^1 \frac{B(s) - B(1) - B'(1)(s-1)}{(1-s)^2} ds. \quad (3.21)$$

Inspection of the exponentially small terms in (3.16) and (3.20) indicates that this expansion is not uniformly valid when $x = O(\varepsilon^{-1})$. This difficulty is easily removed by either a multiple scales approach or, more simply, by using the PLK technique [17]. In this method the leading-order secular behavior is eliminated by replacing ω_0 by ω , where to $O(\varepsilon)$

$$\omega = \omega_0 (1 - (B'(1)/A(1)) \varepsilon + \dots). \quad (3.22)$$

If necessary, a suitable composite solution correct to $O(\varepsilon)$ can be constructed from (3.15), (3.16), (3.18), (3.20) and (3.22). This solution implies that the equilibrium value ($x \rightarrow \infty$) is

$$\alpha_e = 1 - \varepsilon (B(1)/A(1)) + \dots = 1 - \varepsilon \rho_e(1) \exp(1/2\mu_F\phi_e(1)) + \dots, \quad (3.23)$$

in agreement with (3.11). If $\alpha_\infty = \alpha_{e\infty}$ is the limiting value of the mass fraction, then from (3.12) the exact value for the inverse of the decay length is

$$\Omega = \frac{1}{A_\infty} \left(\frac{2 - \alpha_\infty}{\alpha_\infty} \right) \left(1 - \left(\frac{d\alpha_e}{d\alpha} \right)_\infty \right). \quad (3.24)$$

It is straightforward to show that (3.22) is consistent, up to terms $O(\varepsilon)$, with the exact result (3.24).

In Fig. 3 the asymptotic theory is compared with the exact numerical solution for $\varepsilon = 10^{-5}$, $\mu_F = 2$. Employing this value of μ_F is a fairly severe test for the asymptotic limit (see discussion in Sect. 3.3 below), but the agreement is excellent. The final decay law predicted by the PLK value (3.22) gives $\omega \approx 0.597$, and the exact result is $\Omega = 0.589 \dots$

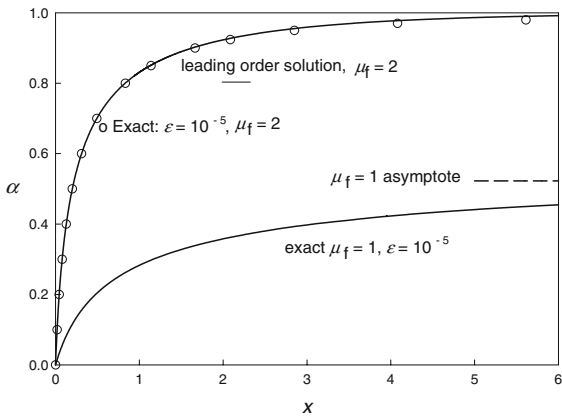


Fig. 3 Small ε theory: $\mu_f > 1$

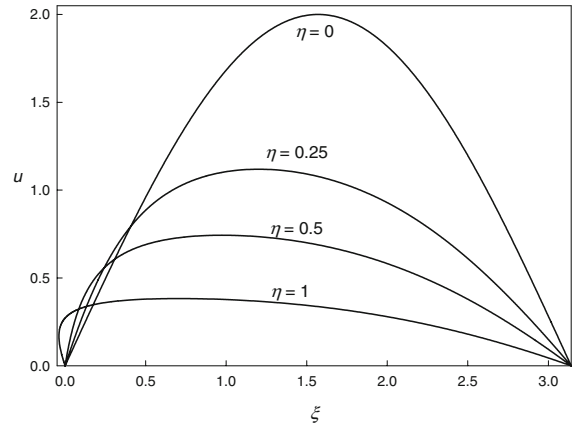


Fig. 4 Sine pulse: decay and shock formation

3.3 Large dissociation density at finite μ_F

When $\mu_F = O(1)$ the final equilibrium value of the mass fraction is not necessarily close to unity. In this case the theory given in Sect. 3.2, which is valid when the dominant decay is controlled by $\alpha \rightarrow 1$, is not valid. Technically, the solution presented in Sect. 3.2 requires that μ_F be large, but as observed above the approach gives excellent results even for $\mu_F = 2$.

In situations where $\alpha_{e\infty} < 1$ with $\mu_F = O(1)$, it is convenient to rewrite the rate law as

$$\frac{d\alpha}{dx} = \varepsilon \rho^3 \left\{ \frac{\alpha_e (1 - \alpha) + \alpha}{1 - \alpha_e} \right\} (\alpha_e - \alpha) \tag{3.25}$$

where factors of λ , $\gamma^{-\frac{1}{2}} M_1^{-1}$ have again been incorporated into the length scale x . This limit corresponds to the numerical data presented in [2]. An example for $\mu_F = 1$ is also shown in Fig. 3.

When $\mu_F \ll 1$, the equilibrium mass fraction is exponentially small. Although suitable results can be obtained, that case is not pursued here.

4 Unsteady wave propagation: near-field limits

4.1 Linear near-field theory

Before discussing the nonlinear near-field theory associated with $\Theta_D \gg 1$ (see Sect. 4.2), it is useful to outline the fully linear theory. Reviews of linear near-field theories for reacting gases can be found in [3, pp. 182–201; 4, pp. 254–281]. Similar near-field results have also been discussed by Chu [6] and by Moore and Gibson [11]. A corresponding equation for visco-elastic materials was derived in [18].

Small disturbance expansions of the form, where δ is an amplitude parameter,

$$\begin{aligned} p &= 1 + \delta p_1(x, t) + \dots, & u &= \delta u_1(x, y) + \dots, \\ T &= T_0 + \delta T_1(x, t) + \dots, & \alpha &= \alpha_0 + \delta \alpha_1(x, t) + \dots, \end{aligned} \tag{4.1}$$

etc.,

lead to a completely linear theory only if $\Theta_D \delta \ll 1$. In (4.1), $T_0 = (1 + \alpha_0)^{-1}$ and α_0 is the initial background (equilibrium) mass fraction. After some algebra it can be shown that for one-dimensional unsteady disturbances the resulting wave equation is

$$\frac{\partial}{\partial t} \left(\frac{\partial^2 T_1}{\partial t^2} - a_0^2 \frac{\partial^2 T_1}{\partial x^2} \right) + \lambda \left(\frac{\partial^2 T_1}{\partial t^2} - a_{e0}^2 \frac{\partial^2 T_1}{\partial x^2} \right) = 0, \tag{4.2}$$

which is the expected classical expression known to govern weak disturbances in a relaxing gas. Here a_0 is the frozen sound speed in the background reference state, and a_{e0} is the corresponding equilibrium sound speed. For convenience, in (4.2) the time and distance scales (t, x) have been replaced by

$$\frac{\varepsilon \alpha_0 (2 - \alpha_0) c_{ve0}}{1 - \alpha_0} \frac{c_{vf}}{c_{vf}} \cdot (t, x) \quad (4.3)$$

where $c_{vf} = (\gamma - 1)^{-1}$ is the frozen specific heat at constant volume, and

$$c_{ve0} = \frac{1}{\gamma - 1} + \frac{\alpha_0 (1 - \alpha_0)}{2 - \alpha_0} \Theta_D^2 (1 + \alpha_0)^2 \quad (4.4)$$

is the corresponding equilibrium value. From the results given in Sect. 2, the frozen sound speed

$$a_0 = \sqrt{\gamma + (\gamma - 1) \alpha_0}, \quad (4.5)$$

but when $\Theta_D \gg 1$ the equilibrium sound speed reduces to the isothermal value

$$a_{e0} = 1. \quad (4.6)$$

Properties of (4.2) have been discussed at length in the literature (see e.g. [3, pp. 182–201; 4, pp. 254–281]).

4.2 Nonlinear near-field theory

If the restriction $\Theta_D \delta \ll 1$ is removed, the small-disturbance results discussed above are no longer valid. The exponential nonlinearity that occurs in the rate law must be retained. Related studies for exothermic reactions have been given in the corresponding large activation energy limit with application to ignition/combustion problems [7]. When $\delta = O(\Theta_D^{-1})$, the expansion (4.1) is replaced by

$$\begin{aligned} p &= 1 + \Theta_D^{-1} (1 + \alpha_0)^{-2} p_1(x, t) + \dots, & \rho &= 1 + \Theta_D^{-1} (1 + \alpha_0)^{-2} \rho_1(x, t) + \dots, \\ T &= T_0 + \Theta_D^{-1} (1 + \alpha_0)^{-2} T_1(x, t) + \dots, & u &= \Theta_D^{-1} (1 + \alpha_0)^{-2} u_1(x, t) + \dots, \\ \alpha &= \alpha_0 + (\gamma - 1)^{-1} \Theta_D^{-2} (1 + \alpha_0)^{-2} \alpha_2(x, t) + \dots, \end{aligned} \quad (4.7)$$

where the factors $(1 + \alpha_0)^{-2}$ and $(\gamma - 1)^{-1}$ have been inserted for later convenience. Note that now, because of the term $\Theta_D \alpha$ in the energy equation, the mass-fraction perturbation is $O(\Theta_D^{-2})$. For clarity, the disturbance is taken to be generated by a small amplitude piston motion and the corresponding initial and boundary conditions are

$$p_1 = \rho_1 = T_1 = u_1 = \alpha_2 = 0 \quad \text{at } t = 0 \quad \text{in } x > 0, \quad (4.8)$$

with

$$u_1 = f(t) \quad \text{on } x = 0 \quad \text{for } t > 0. \quad (4.9)$$

In this section a factor

$$\lambda (\gamma - 1) \alpha_0^2 \varepsilon \Theta_D^2 (1 + \alpha_0)^2 \quad (4.10)$$

is incorporated into the distance and time scales (x, t) , and the signal scale is taken to be comparable to that defined by (4.10). The piston is assumed to accelerate smoothly from rest with $f(0) = 0$, $f'(0) \neq 0$.

From Sect. 2 and the expansion (4.7) the basic form of the governing equations can be written

$$\begin{aligned} \frac{\partial \rho_1}{\partial t} + \frac{\partial u_1}{\partial x} &= 0, & \frac{\partial u_1}{\partial t} + \frac{\partial p_1}{\partial x} &= 0, \\ T_1 + \alpha_2 &= (\gamma - 1) \rho_1, & p_1 &= \alpha_0^2 \rho_1 - (1 + \alpha_0) \alpha_2, \end{aligned} \quad (4.11)$$

$$\frac{\partial \alpha_2}{\partial t} = e^{T_1} - 1.$$

The corresponding evolution equation for the temperature is

$$\frac{\partial}{\partial t} \left(\frac{\partial^2 T_1}{\partial t^2} - a_0^2 \frac{\partial^2 T_1}{\partial x^2} \right) + \left(\frac{\partial^2}{\partial t^2} - \frac{\partial^2}{\partial x^2} \right) e^{T_1} = 0. \quad (4.12)$$

This should be contrasted with the basic linear result (4.2); in 4.12 the rate parameter λ has been included in the time and distance scales. It can be seen that the low-frequency speed takes the isothermal value, and that the low-frequency wave operator acts on the exponential nonlinearity associated with the dissociation rate. Equations of this type have been used to discuss the propagation of weak disturbances in exothermic reacting mixtures and are referred to as Clarke equations [7]. In the exothermic case the sign of the low frequency term is changed and solutions possess logarithmic singularities that correspond to thermal ignition [8,9]. As discussed below, the endothermic (heat loss) form of the Clarke equation leads to a decay of the applied signal.

Other than numerical solutions, a direct analytical attack on (4.12) does not seem possible. Similar remarks apply to the exothermic case, but progress has been made through employment of the Newtonian limit $\gamma \rightarrow 1$ in which the difference between the high- and low-frequency speeds is small [10]. An approach based on the assumption that the sound speeds are close together was used by Moore and Gibson [11] to analyze the endothermic linear equation (4.2). A Newtonian technique is used here to find the solution of (4.12), or more directly to solve the system (4.11). An obvious criterion for the validity of the method is that

$$1 \gg \gamma - 1 \gg \Theta_D^{-1}. \quad (4.13)$$

When $(\gamma - 1) = \Delta \ll 1$, inspection of (4.11) and the initial and boundary conditions (4.8) and (4.9) shows that the leading approximation for the temperature perturbation is simply $T_1 = 0$, and correspondingly $\alpha_2 = 0$. These results imply that the appropriate expansion with respect to Δ has the form

$$p_1(x, t) = p_{10}(x, t) + \Delta p_{11}(x, t) + \dots, \quad T_1(x, t) = \Delta T_{11}(x, t) + \Delta^2 T_{12}(x, t) + \dots, \quad \text{etc.} \quad (4.14)$$

Consequently, in this limit the signalling problem is again linear. The characteristic form of (4.11) is

$$\partial_{0\pm} (p_1 \pm a_0 u_1) = -(1 + \alpha_0) (\partial \alpha_2 / \partial t),$$

with

$$\partial_{0\pm} \equiv \frac{\partial}{\partial t} \pm a_0 \frac{\partial}{\partial x}. \quad (4.15)$$

In (4.15) and subsequent equations it is convenient to retain the full sound speed a_0 , rather than expand about unity. From (4.11), (4.14), and (4.15) it can be seen that the flow field is described by the usual frozen high-frequency relations

$$p_{10} = a_0^2 \rho_{10} = a_0 u_{10} = a_0 f(\xi) \quad (4.16)$$

where

$$\xi = t - x/a_0, \quad (4.17)$$

and $f(t)$ is the applied signal, see (4.9). The leading-order thermal field is governed by

$$\frac{\partial T_{11}}{\partial t} + T_{11} = \frac{\partial \rho_{10}}{\partial t} = \frac{1}{a_0} f'(\xi) \quad (4.18)$$

with

$$\alpha_{21} = \rho_{10} - T_{11}. \quad (4.19)$$

Corresponding solutions satisfying the initial conditions (4.8) are

$$T_{11}(\xi) = a_0^{-1} \int_0^\xi e^{s-\xi} f'(s) ds, \quad \alpha_{21}(\xi) = a_0^{-1} \int_0^\xi e^{s-\xi} f(s) ds. \quad (4.20)$$

(For the imposed signal $f(t) = 0$, $t \leq 0$.)

Evaluation of higher-order terms in the expansion leads to

$$\begin{aligned} u_{11} &= -\frac{1+\alpha_0}{2a_0^2}xT_{11}(\xi), \quad p_{11} = -\frac{1+\alpha_0}{2a_0}xT_{11}(\xi) - \frac{(1+\alpha_0)}{2}\alpha_{21}(\xi), \\ \rho_{11} &= -\frac{1+\alpha_0}{2a_0^3}xT_{11}(\xi) + \frac{(1+\alpha_0)}{2a_0^2}\alpha_{21}(\xi). \end{aligned} \quad (4.21)$$

Similar results can be obtained for $T_{12}(x, t)$ and $\alpha_{22}(x, t)$. In all cases secular terms of the form $x\phi(\xi)$ are observed. These suggest that the expansion fails for $\xi = O(1)$ when t (or x) = $O(\Delta^{-1})$.

Suitable expansions of the form

$$p_1 = \bar{p}_0(\tau, \xi) + \dots, \quad u_1 = \bar{u}_0(\tau, \xi) + \dots, \quad T_1 = \Delta\bar{T}_1(\tau, \xi) + \dots, \quad \alpha_2 = \Delta\bar{\alpha}_1(\tau, \xi) + \dots \quad \text{etc.}, \quad (4.22)$$

are sought. Here

$$\tau = \Delta\left(\frac{1+\alpha_0}{2a_0^2}\right)t, \quad \xi = t - x/a_0. \quad (4.23)$$

(The factor in the definition of τ is for later algebraic convenience.) Substitution in the characteristic equations (4.15) again leads to the standard high-frequency relations

$$\bar{p}_0 = a_0^2\bar{\rho}_0 = a_0\bar{u}_0; \quad (4.24)$$

but now, using the rate and state equations, it can be shown that

$$\frac{\partial\bar{T}_1}{\partial\xi} + \bar{T}_1 = \frac{1}{a_0}\frac{\partial\bar{u}_0}{\partial\xi}, \quad \frac{\partial\bar{u}_0}{\partial\tau} = -a_0\bar{T}_1, \quad \frac{\partial\bar{\alpha}_1}{\partial\xi} = \bar{T}_1. \quad (4.25)$$

Hence \bar{u}_0 satisfies the telegraph equation

$$\frac{\partial^2\bar{u}_0}{\partial\tau\partial\xi} + \frac{\partial\bar{u}_0}{\partial\tau} + \frac{\partial\bar{u}_0}{\partial\xi} = 0. \quad (4.26)$$

From (4.16), matching as $\tau \rightarrow 0$ requires that $\bar{u}_0 \sim f(\xi)$. It follows from (4.26) that (see [11])

$$\bar{u}_0 = e^{-(\xi+\tau)}\frac{\partial}{\partial\xi}\left\{\int_0^\xi I_0\left(2\sqrt{\tau(\xi-s)}\right)e^s f(s)ds\right\}. \quad (4.27)$$

For a pulse of width d , so that $f(t) = 0$, $t \geq d$, it can be established from (4.27) that when $\tau \gg 1$ and $\xi \gg d$ then

$$\bar{u}_0 \sim A\frac{\tau^{\frac{1}{4}}}{\xi^{\frac{3}{4}}}\left(1 + O\left(\frac{1}{\sqrt{\tau\xi}}\right)\right)\exp\left(-(\tau + \xi) + 2\sqrt{\tau\xi}\right), \quad (4.28)$$

where use has been made of the asymptotic behavior of the Bessel function I_0 . In (4.28) the amplitude

$$A = \frac{1}{2\sqrt{\pi}}\int_0^d e^s f(s)ds. \quad (4.29)$$

Equation (4.28) can be simplified further by observing that to leading order

$$\xi - \bar{\xi} = \tau, \quad (4.30)$$

where

$$\bar{\xi} = x - t$$

is the linearized low-frequency characteristic (at high dissociation temperatures the low-frequency equilibrium sound speed reduces to the isothermal value). From (4.29) and (4.30), with $\bar{\xi} = o(\tau)$, it can be shown that

$$\bar{u}_0 \sim A\tau^{-\frac{1}{2}}\exp\left(-\bar{\xi}^2/4\tau\right), \quad (4.31)$$

which, as could be anticipated, is a source solution of the diffusion equation centered on the equilibrium characteristic leaving the origin.

5 High-frequency far-field theory

The analysis described in Sect. 4 did not involve convective nonlinearities. Evolution of these disturbances over large distances can lead to convective steepening of the wave form. Lighthill [5] discussed this effect for near-equilibrium behaviors in a relaxing gas. Implicit in Lighthill’s analysis was the assumption that $\delta\Theta_D \ll 1$. In this section a description of the far-field solution is given for large dissociation energies when $\delta\Theta_D = O(1)$. No assumption is made concerning the magnitude of $\gamma - 1$, but the effective rate parameter (see 4.10)

$$\Lambda = \lambda (\gamma - 1) \alpha_0^2 \varepsilon \Theta_D^2 (1 + \alpha_0)^2 \tag{5.1}$$

is taken to be $O(\Theta_D^{-1})$, which is also the amplitude scale δ ; see (4.7). This provides a suitable distinguished (high-frequency) limit. Nonlinear high-frequency analyses have been given for a relaxing gas at finite characteristic temperatures in [12, 13], and an early treatment of these problems for visco-elastic materials was presented in [19]. Results for exothermic reactions are described in [14, 15]. For the present endothermic case, the solution derived below does not appear to have been previously obtained.

Subject to (5.1), the dominant approximation for the near field is still described by the standard frozen results

$$p_1(x, t) = a_0^2 \rho_1(x, t) = \left(a_0^2 / (\gamma - 1) \right) T_1(x, t) = a_0 u_1(x, t) = a_0 f(\xi_1), \quad \alpha_1(x, t) = 0. \tag{5.2}$$

In (5.2) the factor Λ has not been incorporated into the time and distance scales, and

$$\xi_1 = t - x/a_0 \tag{5.3}$$

is the linearized characteristic associated with the basic scales. Evaluation of higher-order terms using an expansion in Θ_D^{-1} reveals secular behaviors over a distance scale $x = O(\Theta_D^{-1})$ with $\xi_1 = O(1)$. Suitable far field expansions are, with $\Lambda = O(\Theta_D^{-1})$,

$$p = 1 + \Theta_D^{-1} P_1(\xi_1, \eta_1) + \dots, \quad u = \Theta_D^{-1} U_1(\xi_1, \eta_1) + \dots, \quad \alpha = 1 + \Theta_D^{-2} A_1(\xi_1, \eta_1) + \dots, \tag{5.4}$$

with similar expansions for the density and temperature. In (5.4)

$$t = \Theta_D \eta_1. \tag{5.5}$$

As in (5.2) it is found that

$$P_1 = a_0 U_1, \text{ etc. and } U_1 \sim f(\xi_1) \text{ as } \eta_1 \rightarrow 0. \tag{5.6}$$

The characteristic relation associated with the operator ∂_+ then leads to

$$\frac{\partial U_1}{\partial \eta_1} - \left(\frac{a_0^2 + 1}{2a_0} \right) U_1 \frac{\partial U_1}{\partial \xi_1} = - \frac{\Lambda \Theta_D}{2a_0^2 (1 + \alpha_0)} \left[\exp \left((\gamma - 1) (1 + \alpha_0)^2 \frac{U_1}{a_0} \right) - 1 \right]. \tag{5.7}$$

Changing variables through

$$V = (\gamma - 1) (1 + \alpha_0)^2 \frac{U_1}{a_0}, \quad \xi = \frac{(\gamma - 1)^2 (1 + \alpha_0)^3 \Lambda \Theta_D}{a_0^2 (a_0^2 + 1)} \xi_1 = B \xi_1, \quad \eta = \frac{(\gamma - 1) (1 + \alpha_0) \Lambda \Theta_D}{2a_0^2} \eta_1, \tag{5.8}$$

reduces (5.7) to

$$\frac{\partial V}{\partial \eta} - V \frac{\partial V}{\partial \xi} = - \left(e^V - 1 \right). \tag{5.9}$$

By use of (5.8), the initial condition (5.6) becomes

$$V = F(\xi) = (\gamma - 1) (1 + \alpha_0)^2 a_0^{-1} f(\xi/B). \tag{5.10}$$

A related equation has been deduced for the exothermic case by Blythe [14] and by Clarke [15].

Introduction of the characteristic coordinate β through

$$\left. \frac{\partial \xi}{\partial \eta} \right|_{\beta} = -V, \tag{5.11}$$

and taking $\xi = \beta$ at $\eta = 0$, enables the solution of (5.11) to be written in parametric form as

$$V = -\log \left[1 - e^{-\eta} \left(1 - e^{-F(\beta)} \right) \right], \quad (5.12)$$

and

$$\xi = \beta + \int_0^\eta \log \left[1 - e^{-s} \left(1 - e^{-F(\beta)} \right) \right] ds. \quad (5.13)$$

Solutions of this type are not necessarily unique. The evolution of the sine pulse

$$F(t) = \begin{cases} 2 \sin t, & 0 \leq t \leq \pi, \\ 0, & t > \pi, \end{cases} \quad (5.14)$$

is shown in Fig. 4; clearly, the solution for $\eta = 1$ is no longer single-valued. Obtaining the appropriate single-valued solution requires the insertion of suitable Rankine–Hugoniot shock waves. In general, difficulties with the solution represented by (5.12) and (5.13) will arise when

$$\partial \xi / \partial \beta|_\eta = 0.$$

It can be shown that these points are defined by

$$e^\eta = \frac{e^{F(\beta)} - 1}{e^{F(\beta)} - \exp\left(\frac{e^{F(\beta)} - 1}{F'(\beta)}\right)}. \quad (5.15)$$

If both F and F' are initially positive, then (5.15) will yield solutions with $\eta > 0$ provided that

$$F' > F^{-1} \left(e^F - 1 \right). \quad (5.16)$$

If the smallest value of η occurs on the front, a shock will originate there with

$$\eta_{0s} = \log \left(\frac{F'(0)}{F'(0) - 1} \right) \quad (5.17)$$

provided that $F'(0) > 1$. For the example shown in Fig. 4, the shock will originate on the front at $\eta = \log 2$.

From the shock relations (in which the right hand sides in (3.3) are replaced by appropriate local values with $[\alpha] = (0)$) it can be established for the weak limit corresponding to (5.9) that the shock path is governed by

$$\frac{d\xi_s}{d\eta} = -\frac{1}{2} (V_+ + V_-). \quad (5.18)$$

Here V_+ and V_- denote the values at the shock on the characteristics β_+ and β_- that meet on either side of the shock. In cases where the shock forms at the front, as in (5.13), the results (5.12), (5.13), and (5.18) can be used to show that on the shock path

$$V \frac{d\eta_s}{d\beta} = 2 \left\{ 1 + \frac{F'}{e^F - 1} (V - F) \right\}, \quad (5.19)$$

where V is defined by (5.12) with $\eta = \eta_s$. This equation is to be solved subject to

$$\eta = \eta_{0s} \quad \text{at } \beta = 0, \quad (5.20)$$

and the parametric description of the shock path is completed by obtaining $\xi_s(\beta)$ from (5.13) with η replaced by η_s . The shock path for the pulse (5.14) is shown in Fig. 5.

A suitable measure of the shock strength is the scaled velocity V immediately behind the shock, and this quantity is displayed in Fig. 6 for the profile (5.14). As $\eta \rightarrow \infty$, the final decay is defined by

$$V_s \sim \xi_s - \xi_\infty \sim (1 - F(\beta_\infty)) e^{-\eta}, \quad (5.21)$$

where ξ_∞ and β_∞ are the constant limiting values of ξ and β , respectively.

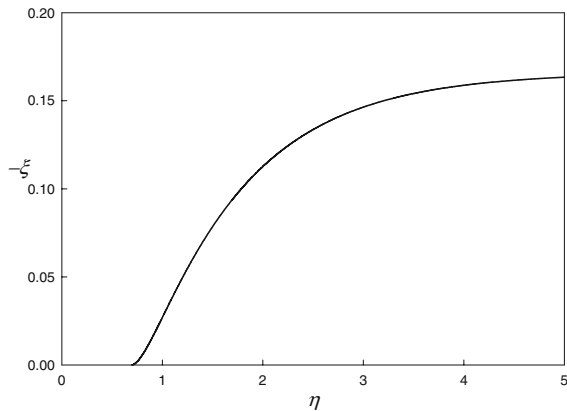


Fig. 5 Shock path for a sine pulse

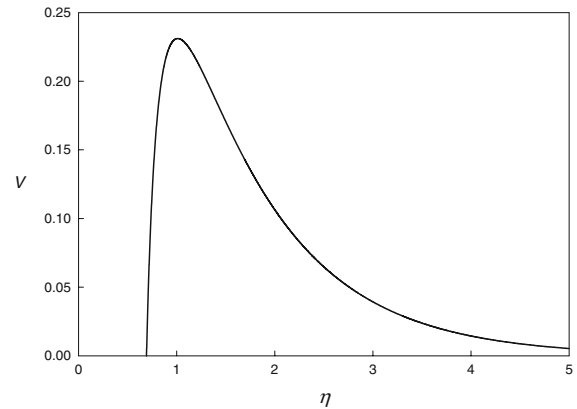


Fig. 6 Shock decay for a sine pulse

6 Concluding remarks

The simple ideal dissociating-gas model introduced by Lighthill [1] has proved to be an excellent tool for investigating the basic structure of continuum non-equilibrium high-temperature gas flows. For the principal constituents of air, nitrogen and oxygen, characteristic dissociation temperatures Θ_D and dissociation densities ρ_D are usually, in an appropriate dimensionless sense, large. Freeman [2] exploited the large dissociation-temperature limit in describing shock structure at hypersonic speeds. In Sect. 3, these results were extended to larger values of the Freeman parameter $\mu_F = \gamma M_1^2 / 2\Theta_D$, or equivalently, to larger values of the shock Mach number M_1 .

Other early work that exploited $\Theta_D \gg 1$ was concerned with expanding flows [20–22]. Although not discussed here, these analyses examined supersonic nozzle flows in which the dissociation mass fraction freezes at some fixed level well above the local equilibrium value α_e . This strong departure from equilibrium can have a marked effect on working section (test) conditions, and can lead to a significant loss of thrust in rocket engines. Judicious choices of the dimensionless dissociation density and the rate parameter can generate frozen levels for which $\alpha = O(1)$, even though $\alpha_e \ll 1$, [22]. Two-dimensional numerical solutions for expansion corners have been obtained and the general properties are known, (see e.g. [23]), but the detailed structure of these flows could be investigated based on the large dissociation energy limit.

Most of the present paper has been concerned with wave propagation in an ideal dissociating gas when $\Theta_D \gg 1$. Again, parameter limits were considered in which the local mass fraction $\alpha = O(1)$, but now α_e is also $O(1)$. As noted in Sect. 4b, even when the wave amplitude is small, exponential nonlinearities associated with the chemistry must be taken into account. In the near field, disturbances are governed by an endothermic Clarke equation [7]. A discussion of the solution of this equation was given for the Newtonian limit $\gamma \rightarrow 1$. In this limit, for which the high- and low-frequency sound speeds are close together, it was shown that the large time asymptotic behavior is equivalent to a diffusive source centered on a low-frequency characteristic. For the high-dissociation-temperature limit, the equilibrium (low-frequency) sound speed reduces to the isothermal value (see Sect. 2). In general, even for small amplitude signals, convective nonlinearities can affect the far field behavior. A discussion of weakly nonlinear signalling problems is given in Sect. 5 for the distinguished limit when $\delta = O(\Theta_D^{-1})$, where δ is a dimensionless measure of the signal amplitude. Only high-frequency signals are considered, i.e., the frequency of the applied signal is large compared with the frequency defined by the effective relaxation time. The governing equation (5.9) contains both convective and exponential nonlinearities, and the general solution is given in Sect. 5. An example is presented there for the evolution of a compressive sine pulse, including the formation and evolution of a shock that develops on the pulse front. Far-field behavior over a broader frequency range, in both expansive and compressive flows, should be amenable to a large-dissociation-temperature analysis. For this limit, it would also be interesting to

examine fully dispersed structures in which the diffusive effects of the rate process completely balance convective steepening. A basic description of steady fully dispersed shock structure was presented by Lighthill [5].

Acknowledgements It is a pleasure to dedicate this paper to the memory of James Lighthill. I was a student at the University of Manchester, both undergraduate and graduate, at the time when James was Head of Applied Mathematics. His undergraduate lectures were models of all that this form of instruction should be. In particular, I recall his final-year course on Thermodynamics which, in true Lighthill style, ranged from classical theory to statistical mechanics. Before deciding on graduate school, I sought employment in the aircraft industry. One of my interviewers started by asking me what I knew about dissociating gases. My reply of “Not much” was met with the response, “But you must, Lighthill is at Manchester.” This lack of acquaintance with matters reacting and relaxing was changed dramatically on entering graduate school and reading James’s papers on these topics. Again, they were models of their kind.

References

1. Lighthill MJ (1957) Dynamics of a dissociating gas. Part I. Equilibrium flow. *J Fluid Mech* 2:1–32. doi:[10.1017/S0022112057000713](https://doi.org/10.1017/S0022112057000713)
2. Freeman NC (1958) Non-equilibrium flow of an ideal dissociating gas. *J Fluid Mech* 4:407–425. doi:[10.1017/S0022112058000549](https://doi.org/10.1017/S0022112058000549)
3. Clarke JF, McChesney M (1964) *The dynamics of real gases*. Butterworths, London
4. Vincenti WG, Kruger CH Jr (1965) *Introduction to physical gas dynamics*. Wiley, London
5. Lighthill MJ (1956) Viscosity effects in sound waves of finite amplitude. In: Batchelor GK, Davies RM (eds), *Surveys in mechanics*. Cambridge University Press, Cambridge
6. Chu BT (1957) Wave propagation and the method of characteristics in reacting gas mixtures with applications to hypersonic flow. Wright Air Development Center TN-57–213
7. Clarke JF (1981) Propagation of gas dynamic disturbances in an explosive atmosphere. *Prog Astronaut Aeronaut* 76:383–402
8. Clarke JF, Cant RS (1985) Nonsteady gasdynamic effects in the induction domain behind a strong shock wave. *Prog Astronaut Aeronaut* 95:142–163
9. Jackson TL, Kapila AK (1985) Shock induced thermal runaway. *SIAM J App Math* 49:432–458. doi:[10.1137/0149027](https://doi.org/10.1137/0149027)
10. Blythe PA, Crighton DG (1989) Shock-generated ignition: the induction zone. *Proc R Soc Lond A Math Phys Sci* 426:189–209. doi:[10.1098/rspa.1989.0123](https://doi.org/10.1098/rspa.1989.0123)
11. Moore FK, Gibson WE (1960) Propagation of weak disturbances in a gas subject to relaxation effects. *J Aerospace Sci* 27:117–127
12. Blythe PA (1969) Non-linear wave propagation in a relaxing gas. *J Fluid Mech* 37:31–50. doi:[10.1017/S0022112069000401](https://doi.org/10.1017/S0022112069000401)
13. Ockendon H, Spence DA (1969) Non-linear wave propagation in a relaxing gas. *J Fluid Mech* 39:329–345. doi:[10.1017/S0022112069002205](https://doi.org/10.1017/S0022112069002205)
14. Blythe PA (1979) Wave propagation and ignition in a combustible mixture. Proc. 17th int. symp. on combustion, The Combustion Institute, Pittsburgh, PA, 909–916
15. Clarke JF (1979) On the evolution of compression pulses in an exploding atmosphere: initial behaviour. *J Fluid Mech* 94:195–208. doi:[10.1017/S0022112079000999](https://doi.org/10.1017/S0022112079000999)
16. Johannesen NH (1961) Analysis of vibrational relaxation regions by means of the Rayleigh-line method. *J Fluid Mech* 10:25–32. doi:[10.1017/S0022112061000032](https://doi.org/10.1017/S0022112061000032)
17. Lighthill MJ (1949) A technique for rendering approximate solutions to physical problems uniformly valid. *Philos Mag* 40:1179–1201
18. Morrison JA (1957) Wave propagation in rods of Voigt material and visco-elastic materials with three parameter models. *Q App Math* 14:153–169
19. Varley E, Rogers TG (1967) The propagation of high-frequency finite acceleration pulses and shocks in visco-elastic materials. *Proc R Soc Lond A Math Phys Sci* 296:498–518. doi:[10.1098/rspa.1967.0041](https://doi.org/10.1098/rspa.1967.0041)
20. Bray KNC (1959) Atomic recombination in a hypersonic wind tunnel nozzle. *J Fluid Mech* 17:1–32. doi:[10.1017/S0022112059000477](https://doi.org/10.1017/S0022112059000477)
21. Blythe PA (1964) Asymptotic solutions in non-equilibrium nozzle flow. *J Fluid Mech* 20:243–272. doi:[10.1017/S0022112064001185](https://doi.org/10.1017/S0022112064001185)
22. Cheng HK, Lee RS (1968) Freezing of dissociation and recombination in supersonic nozzle flows: part I. General discussion and special analysis. *AIAA J* 6:823–837. doi:[10.2514/3.4605](https://doi.org/10.2514/3.4605)
23. Appleton JP (1963) Structure of a Prandtl-Meyer expansion in an ideal dissociating gas. *Phys Fluids* 6:1057–1062. doi:[10.1063/1.1706862](https://doi.org/10.1063/1.1706862)